Solar and Stellar Variability: Impact on Earth and Planets
Proceedings IAU Symposium No. 264, 2009
A. G. Kosovichev, A. H. Andrei & J.-P. Rozelot, eds.

doi:10.1017/S1743921309992869

Are there variations in Earth's global mean temperature related to the solar activity?

Olav Kjeldseth-Moe[1] **and Sven Wedemeyer-Böhm**[2]

[1]Institute of Theoretical Astrophysics, University of Oslo, Oslo, Norway
email: `olavm@astro.uio.no`

[2]Institute of Theoretical Astrophysics, University of Oslo, Oslo, Norway
email: `sven.wedemeyer-bohm@astro.uio.no`

Abstract. We have analyzed the record of Earth's global temperature variations between 1850 and 2007 looking for signals of periodic variations and compared our results with solar activity variations in the same time period. Significant periods are found at 9.4, 10.6 and 20.9 years. These periodic variations may be caused by solar activity. However, and amazingly enough, we also find at least 17 other significant periodic variations in addition to expected variations with periods of 1 year and of half a year. The result is considered in terms of solar related forcing mechanisms. These may be variable solar heating associated with the small changes in solar irradiance over the solar cycle, or direct effects of interactions between variable magnetic fields carried by the solar wind and particles and fields in interplanetary space or in the Earth's ionosphere.

Keywords. Earth: global temperature, Sun: activity

---

1. Introduction

The role of solar forcing on Earth's global temperature level is a disputed question. In addition to radiative forcing, which is weak, it has been suggested that variations in the influx of cosmic rays into interplanetary space, owing to solar magnetic activity, causes variations in cloud formation on Earth that may account for climate changes on long timescales, from years to millennia (e.g. Svensmark 2007). However, other magnetically related effects are also conceivable.

Looking for periods in the global temperature on the same time scale as solar activity variations may thus be a way of checking on the amount and character of solar forcing, whether thermal or magnetic. Any periodic variations may, so to speak, serve as a calibration for solar effects. We have therefore analyzed the record of Earth's global temperature between 1850 and 2007 looking for periodic signals in the range 1–30 years. To establish a good average value for the solar activity period in the same time interval, we also analyzed the record of sunspot numbers, taking these as a satisfactory indicator of solar magnetic variations, causing variations in the spectrally integrated solar irradiance as well as interacting with magnetic fields on Earth and in space around us.

2. Data sources and data reduction

The data consist of the record of Earth's global temperature variation together with solar activity data for the period 1850 through 2007, i.e. 158 years.

Solar activity. The significance of the solar activity variations is twofold. Firstly, a small variation in the irradiance with solar activity has been found from three decades of space observations (see e.g. Fröhlich 2006, Scafetta 2009 and references therein). An absolute calibration of the variable solar irradiance is problematic, but clearly its peak-to-peak variation is ≈1 W m^{-2}, with an average value near 1366 W m^{-2}, i.e. a total variation of 0.075 percent. Secondly, the transport of magnetic fields from the Sun into interplanetary space increases strongly with increasing solar activity. This may influence cloud formation on Earth, according to Svensmark (2007), or affect tropical electric storm activity with further effects on global temperatures.

To find the length of the solar activity cycle we used daily sunspot numbers listed by the Solar Influences Data Analysis Center, Royal Observatory of Belgium, (see SIDC: http://www.sdic.be/sunspot-data). A recent thorough analysis of these data was made by Gil-Alana(2009). He obtained a value for the period of 130 months, or 10.83 years, for the interval 1749–2008. However, in the first century of this interval the sunspot record is incomplete.

We therefore performed a Fourier analysis of the data in the 158 year interval referred to above and found a value for the period of 10.45 ± 0.6 years. The given uncertainty is simply estimated from the width of a Gaussian fit to the slightly asymmetrically placed power spectrum peak corresponding to the 11 year period.

Global temperatures. Global temperatures are taken from the United Kingdom Met Office Hadley Centre observations datasets. A table of monthly and annual temperature anomalies, i.e. global temperatures in °C relative to a mean over a range of years, is listed in the HadCRUT3 database (see http://hadobs.metoffice.com/hadcrut3/). Formats of the HadCRUT3 tables can be obtained from the same site. Regarding the formats we note that the data tables, in addition to the most reliably estimated anomalies, also contain the upper and lower 95% uncertainty ranges from the combined effects of all uncertainties. The data and uncertainties are described by Brohan *et al.* (2006).

In our investigation we shall use the monthly temperature anomalies. The best monthly anomalies from 1850 through 2007 as listed in the HadCRUT3 database, are shown in the left panel of Figure 1.

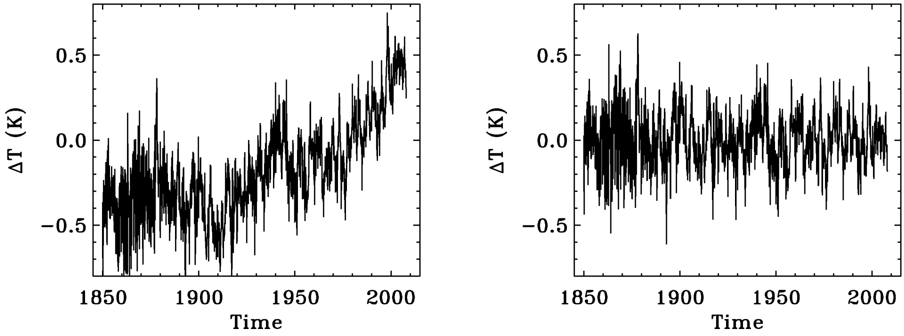

Figure 1. Left panel: Global temperature anomaly 1850–007. Right panel: Temperature anomaly with long term trends subtracted and average equal to zero.

Before we analyzed the data we subtracted long-term trends. For this we fitted a high order polynominal to the observed anomalies and subtracted the time series values obtained from the polynominal. We found that a 10th order polynominal gave the lowest chi-square value for the fit. Afterwards we subtracted the very small average of the resulting anomalies (≈ 10^{-4} °C). This removed the zero frequency power from the power spectrum and facilitated detection of periods of the order 10-20 years. The procedure only adds a small uncertainty to the lowest frequencies, f = 1–5. The result, which we shall call the differential temperature anomaly, is shown in the right panel of Figure 1.

Power spectrum and significance of power signals. The monthly differential temperature anomalies have been Fourier analyzed and the power spectrum calculated. The result is shown in Figure 2. We have limited the plot to the 170 lowest frequencies. A yearly variation is clearly present at f=158. In addition there is a likely significant peak at f=316, i.e. corresponding to a half-yearly variation.

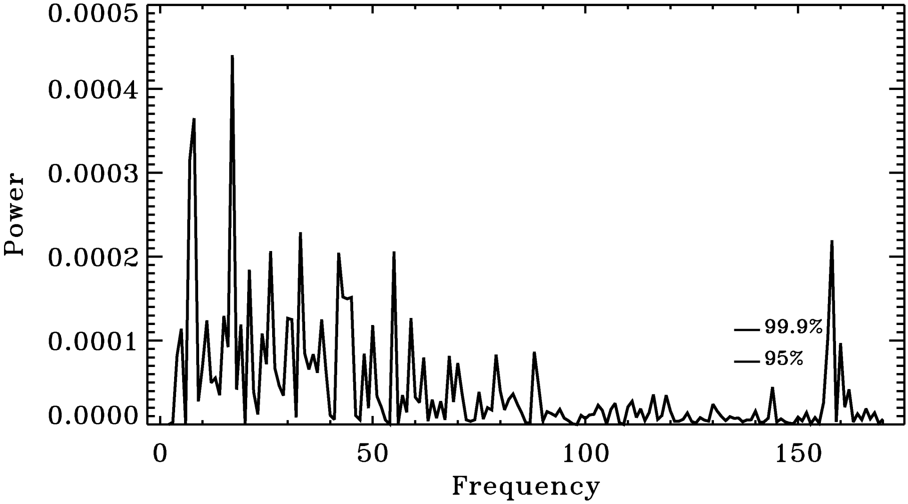

Figure 2. Power spectrum of the differential global temperature anomaly, for f = 0–170.

Two annotated marks in the figure give power levels where we find that given fractions of power values above these levels correspond to real signals and are not caused by noise. Thus, for power values larger than 7.5 10^{-5} and 1.1 10^{-4} the fraction of real signal values relative to the total number of noise and signal together is 95 % and 99.9 %, respectively. We shall now describe how we have estimated this significance of any particular power value, something that is needed in order to decide which of the peaks in the power spectrum correspond to real time variations, as distinguished from noise.

The noise level in the power spectrum of a data set may be estimated by shuffling the data randomly and calculate the power spectrum of the shuffled data. If this is done many times, say a 1000 times or more, a significant average is obtained. The procedure gives a reasonable result if the power in the data is dominated by the noise, which is the case here. However, there is always an amount of signal mixed into the noise obtained this way.

The significance of a particular power value may, however, be estimated in another fashion. If we plot the distribution of values in our power spectrum we get a normalized distribution function as shown in the left panel of Figure 3. The normalized distribution, $N(p)/N$, is defined as the number of values per power unit in the power spectrum as a function of power, p. It is obtained by dividing the power spectrum into small sections each covering a range in power from p to p+δp, counting the number of values in each section, and dividing by the interval δp. The crosses in the figure give the counted values while the drawn line is the best estimate of a curve through the points. This curve consists of two exponential functions added together, where the exponents are linear functions of power, p. Thus, they appear as straight lines on the logarithmic scale of the y-axis.

The two separate domains for high and low powers correspond to a noise dominated and a signal dominated part of the distribution function. A synthetic model may easily demonstrate this. Thus, we made a data set of 20 oscillation with different amplitudes and with frequencies close to the probable frequencies in the power spectrum of the real data. Then we added different amounts of noise to the resulting time series values. The result is seen in Figure 3b, where two of the curves have noise levels bracketing what is found in the real data and the third curve (dot-dashed) is from the synthetic data set with no noise at all. We did not include the counted values in the plots in Figure 3b, but they correspond in a general fashion to the counted values in the analysis of real temperature data shown in the left panel, Figure 3a.

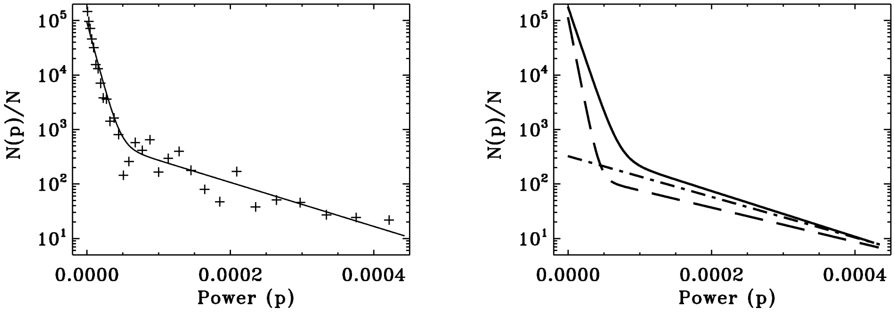

Figure 3. Left panel (a): Normalized distribution of power values in the power spectrum of Earth's differential global temperature anomalies. Right panel (b): Normalized distribution of power values in the power spectrum of a synthetic set of 20 oscillations, with different levels of noise added.

The likelihood of a particular power value being caused by a real signal or by noise may then be derived from the two contributing distributions in Figure 3a. This is how the fractional annotation values in Figure 2 were determined. Uncertainties in the derived likelihood values may furthermore be computed from the uncertainties in the fitting of straight lines to the logarithm of the "noise" and the "signal" distributions, respectively, in the two domains in Figure 3a.

Finally, the values of the power peaks (and indeed any value in the power spectrum) have uncertainties owing to the inherent total uncertainty of the given temperature anomalies. The 95% uncertainty ranges from the combined effects of all the uncertainties are, as mentioned above, included in the data set. The uncertainties may not be randomly distributed, but for our purpose we have assumed this as a sufficiently close approximation. A large number (30000) of time series of possible temperature anomalies were created, where Gaussian randomly distributed increments were added to each temperature value in the original best series. These random temperature increments were all different, had a mean of zero and a standard value corresponding to the given uncertainties in the measured temperature anomalies. Thus, the 95% limits were regarded as 2 × sigma deviations from a mean value. The synthetic temperature anomalies were then treated the same way as the standard set of values and their power spectra were derived. From this we obtained the distribution of the power in the power spectrum. An example, including the two strong power peaks at f=7-8 and f=17 and a selection of four other peaks in the power spectrum, is shown in Figure 4. The values for the 95% and 99% likelihood of the power peak being caused by a real signal is marked in the figures (broken vertical lines).

3. Results

The results of the investigation are presented in Figure 2 and in Table 1. In Table 1 we list parameters for oscillations with power values larger than $0.85 \cdot 10^{-4}$. Power values at this lower limit are significant to 95%, even if the uncertainty in the limit is taken into account. Most of the listed power peaks can, however, be considered as real signals with a significance of well above 99.9%.

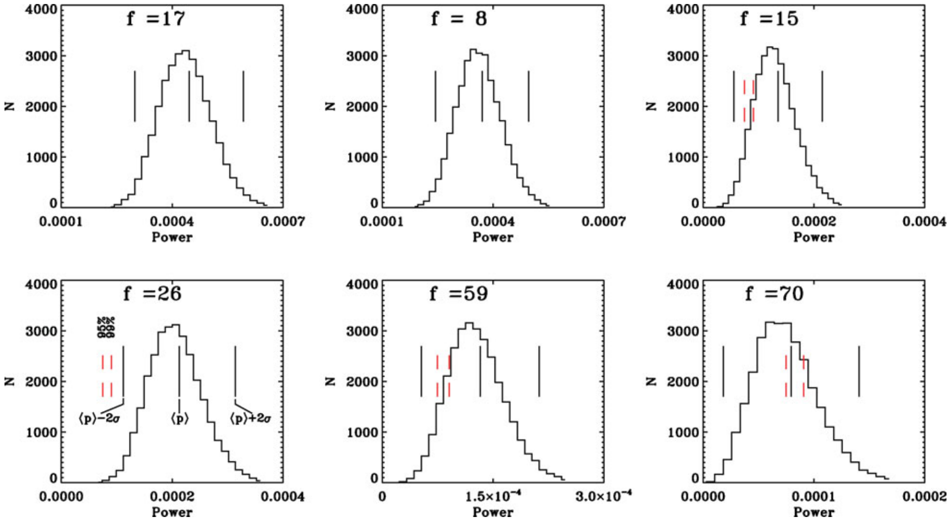

Figure 4. Distribution of power values at 6 selected frequencies derived from the uncertainties in the observed temperature anomalies, 1850–2007. $< p >$ is the average power value.

Table 1. The strongest maxima in the global temperature power spectrum.

Frequency (nominal)	Frequency–f_a (adjusted)	Power value (at peak x 10^4)	Period (years)	Remarks
(4)-5	4.60	1.18 ± 0.30	34.4	Asymmetric feature
(7)-8	7.56	3.70 ± 0.63	20.9	Asymmetric feature
11	10.87	1.30 ± 0.39	14.5	
15	14.90	1.36 ± 0.39	10.6	
17	16.90	4.45 ± 0.72	9.35	
19	18.75	1.25 ± 0.39	8.42	
21	21.21	1.90 ± 0.48	7.45	
24	24.29	1.14 ± 0.37	6.51	
26	25.98	2.13 ± 0.51	6.08	
30-31		1.27	5.2	Blended feature
33	33.24	2.29 ± 0.5	4.75	
38	38.02	1.31 ± 0.40	4.16	
42-45		2.15	3.75-3.5	Broad blended feature
48	48.11	0.91 ± 0.33	3.28	
50	50.07	1.25 ± 0.39	3.15	
55	55.01	2.12 ± 0.51	2.87	
59	59.11	1.32 ± 0.40	2.67	
62	61.80	0.86 ± 0.32	2.56	
68	68.17	0.88 ± 0.32	2.32	
79	79.21	0.89 ± 0.32	1.99	
158	157.68	2.25 ± 0.53	1.00	
160	160.14	1.03 ± 0.35	0.987	
316	315.93	0.90 ± 0.34	0.50	

We start by noting that the two strongest periods in the power spectrum are located at nominal frequencies f=8 and f=17. These peaks are unequivocally caused by a real signal. They are clearly outstanding also if we analyze the annually averaged temperature anomalies. In addition there is a weaker power peak at f=15, blended in with the stronger peak at f=17. Table 1 gives more accurate frequencies, found by fitting Gaussians to the sometimes asymmetrically placed power peaks and deriving the position of these profiles. The periods of oscillations corresponding to f=8, 15 and 17, are 20.9 ± 1.7 years, 10.60 ± 0.42 years, and 9.35 ± 0.35 years, respectively. Periods are determined from the expression $P = 158/f_a$, since the data set is 158 years long. Uncertainties in the periods are estimated from an assumed full width at half maximum (FWHM) of the power peaks of 1 frequency unit. The periods of f=8 and f=15 agree especially well with the solar activity period of 10.45 ± 0.6 years and with twice this period, which correspond to the periodic variation of the changing solar magnetic polarity. The temperature amplitudes of the three oscillations are approximately 0.05 K, 0.035 K and 0.05 K, respectively.

The investigation started as a search for periodicities corresponding to the solar activity period. However, the detection of a number of other persistent and clearly significant periods, came as a serendipitous, amazing and exciting additional result. Periods of half a year, one year, and two years, are clearly related to the Earth, moving in its eccentric orbit around the Sun, and having different distributions of continents and oceans on the two hemispheres. The other oscillations have periods shorter than ≈ 9 years, with exception of one period at 34 years. It seems likely that these variations persist over long times, since the global mean temperature data span almost 160 years.

4. Concluding remarks

The closeness in period between the strongest global temperature variations and the period of solar activity points to a clear connection between the two. The 21 year period might possibly be an undertone of the shorter period variation and might thus be caused by solar irradiance variations. However, a mechanism depending on solar magnetic polarity regulating how well solar wind particles penetrate the Earth's magnetosphere, would also have to be considered. Whether solar irradiance variations would be able to drive oscillations with the derived temperature amplitudes is also an open question, but may at a first glance seem likely. But what about all the other persistent oscillations in the global temperatures? They also have to be driven by an external variable energy input. Also here the ultimate driving force may be solar variations, but perhaps the required energies from irradiance variations alone are insufficient. These and other questions will be addressed in ongoing investigations.

References

Brohan, P., Kennedy, J. J.., Harris, I., Tett, S. F. B., & Jones, P. D. 2006, *Geophys. Res.*, 111, D12106

Fröhlich, Claus 2006, *Space Science Reviews*, 125, 531

Gil-Alana, Luis A. 2009, *Solar Phys.*, 257, 371

Scafetta, Nicola 2009, *arXiv:0908.0792S [astro-ph.SR] 6 Aug 2009*

Svensmark, Henrik 2007, *Astronomy and Geophysics*, 48, 1.18